



**HAL**  
open science

## Relaxation of a Grooved Profile Cut in a Crystalline Surface of High Symmetry

Erwan Adam, Anna Chame, Frédéric Lançon, Jacques Villain

► **To cite this version:**

Erwan Adam, Anna Chame, Frédéric Lançon, Jacques Villain. Relaxation of a Grooved Profile Cut in a Crystalline Surface of High Symmetry. *Journal de Physique I*, 1997, 7 (11), pp.1455-1473. 10.1051/jp1:1997141 . jpa-00247463

**HAL Id: jpa-00247463**

**<https://hal.science/jpa-00247463>**

Submitted on 4 Feb 2008

**HAL** is a multi-disciplinary open access archive for the deposit and dissemination of scientific research documents, whether they are published or not. The documents may come from teaching and research institutions in France or abroad, or from public or private research centers.

L'archive ouverte pluridisciplinaire **HAL**, est destinée au dépôt et à la diffusion de documents scientifiques de niveau recherche, publiés ou non, émanant des établissements d'enseignement et de recherche français ou étrangers, des laboratoires publics ou privés.

# Relaxation of a Grooved Profile Cut in a Crystalline Surface of High Symmetry

Erwan Adam (\*), Anna Chame (\*\*), Frédéric Lançon and Jacques Villain (\*\*\*)

Département de Recherche Fondamentale sur la Matière Condensée, CEA Grenoble,  
38054 Grenoble Cedex 9, France

(Received 17 February 1997, revised 19 June 1997, accepted 27 June 1997)

PACS.68.35.Bs – Surface structure and topography

PACS.68.35.Ja – Surface and interface dynamics and vibrations

PACS.02.70.Lq – Monte Carlo and statistical methods

**Abstract.** — The smoothing of artificial grooves on a high-symmetry crystal surface below its roughening transition is investigated in the light of a one-dimensional model. In the case of diffusion dynamics, a new, kinetic, attractive interaction between steps opposes the contact repulsion and tends to flatten the top and the bottom of the profile in the transient state anterior to complete smoothing. This phenomenon, which is absent from continuum models, is weaker, but still present in real, two-dimensional surfaces.

Kinetic Monte Carlo simulations have been performed for large modulation amplitudes in contrast with previous works. The relaxation time  $\tau$  scales with the wavelength  $\lambda$  as  $\tau \propto \lambda^3$  for diffusion dynamics and as  $\tau \propto \lambda^2$  for evaporation dynamics. In the case of evaporation dynamics, the transient profile is sinusoidal. In the case of surface diffusion the profile presents blunted parts at the top and at the bottom, which result from the kinetic attraction between steps.

## 1. Introduction

The smoothing of grooves artificially made in a crystal surface is a classical problem [1–3] solved by Mullins [5] in the case of a non-singular surface. Mullins's theory predicts that the shape of the profile will remain sinusoidal during the relaxation and that its amplitude will decrease exponentially with the time.

In the present paper, we address the case of singular (001) and (111) faces, below their roughening transition temperature, when the profile can be appropriately described as an alternation of steps and terraces [6, 7]. Experimentally, a transient state is observed where facets form at maxima and minima before the grooves smooth out [2–4]. Such facets are not expected from the theoretical analyses of Rettori and Villain [6] and Ozdemir and Zangwill [7] except if the surface is miscut [10, 11], as it is in practice. However, the figures obtained by

---

(\*) Author for correspondence (e-mail: adam@drfmc.ceng.cea.fr)

(\*\*) *Permanent address:* Instituto de Física, Universidade Federal Fluminense, 24210-340, Niterói RJ, Brazil

(\*\*\*) *Alternative address:* Centre de Recherches sur les Très Basses Températures-CNRS, BP 166, Grenoble Cedex 9, France

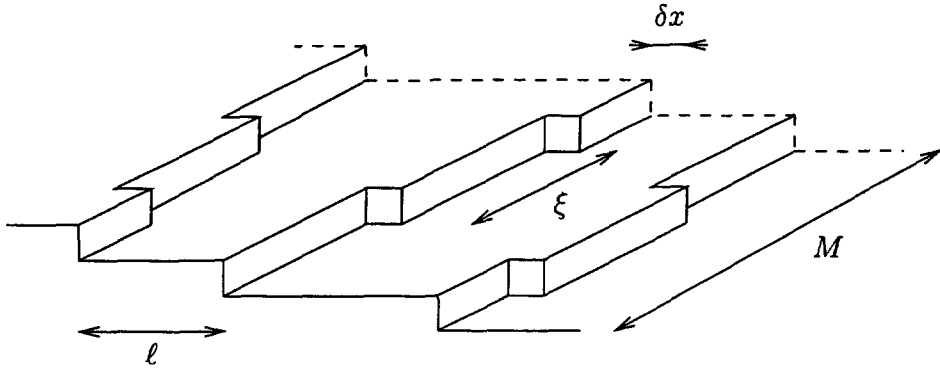


Fig. 1. — Steps of length  $M$  separated by a distance  $\ell$ . The typical distance between kinks along a step is  $\xi$ , and each step can fluctuate in a distance  $\delta x$ .

simulations of Jiang *et al.* [15,16] do show facets even for a well cut surface, in agreement with some theoretical models [8,9].

The main problem in simulations [14–17] is that the systems considered are small in the three directions. Indeed, in order to obtain the correct scaling laws (*e.g.* the relaxation time  $\tau$  *vs.* the wavelength  $\lambda$ ), the amplitude  $h$  and the average distance between steps  $\ell = a\lambda/(4h)$  must be large with respect to the atomic distance  $a$ .

The problem related to the width  $M$  of the system in the direction of the grooves is different. In available analytical or numerical theories, elastic or electrostatic interactions between the steps which form the profile are not considered, and then the only interaction which remains is the contact repulsion. In analytic theories [6–9] this contact repulsion is taken into account by introducing an effective free energy equal [12,13] to

$$F_{\text{ent}} = M \frac{(\pi k_{\text{B}} T)^2}{6\gamma \ell^2} \quad (1.1)$$

for each pair of steps at average distance  $\ell$ . Here,  $\gamma$  is the line stiffness related to the energy  $W$  per kink by the relation

$$\beta\gamma a = 1 + \frac{\exp(\beta W)}{2} \quad (1.2)$$

where  $\beta = 1/k_{\text{B}}T$ .

Formula (1.1) is correct only for long distances  $\ell$ . Moreover, as noted by Murty and Cooper [18], (1.1) makes sense only for large  $M$  (see condition (2.3)). The purpose of this article is to study the case of short samples, with small values of  $M$ , while all other lengths ( $h$ ,  $\lambda$ ) are much larger than  $a$ .

## 2. What is a Short Sample?

More precisely, the average distance between kinks along a step is (Fig. 1)

$$\xi \approx a \left( 1 + \frac{\exp(\beta W)}{2} \right). \quad (2.1)$$

Thus, the average square end-to-end deviation of an isolated step of length  $M$  with respect to its average position is

$$\langle \delta x^2 \rangle = \frac{2 \exp(-\beta W)}{1 + 2 \exp(-\beta W)} M a \cong \frac{M a^2}{\xi} \quad (2.2)$$

where  $x$  denotes the direction perpendicular to the groove direction (or to the average step direction) on the surface. Formula (2.2) is expected to hold if steps are so far apart that  $\langle \delta x^2 \rangle \ll \ell^2$ , i.e.  $M \ll \xi \ell^2 / a^2$ , so that contact interactions between steps are not relevant.

An exact calculation [19] — for instance considering a single fluctuating line between two straight lines at distance  $2\ell$  [20] — shows that (1.1) holds only if the opposite relation

$$M \gg \xi \left( \frac{\ell}{a} \right)^2 \quad (2.3)$$

is satisfied. This yields a first condition on  $\xi$

$$\xi \ll M \left( \frac{4h}{\lambda} \right)^2 \quad (2.4)$$

Whether this condition is satisfied or not depends on the temperature  $T$ , which should anyway be smaller than  $T_R$ . An order of magnitude of  $T_R$  is given by writing that the free energy of an isolated step per atom, which is  $W - k_B T \ln[1 + 2 \exp(-\beta W)]$  at low temperature, vanishes. Thus

$$\exp \frac{W}{k_B T_R} = 2. \quad (2.5)$$

As a matter of fact, if one wishes to check the analytic predictions made for singular surfaces, it is safer to choose  $T$  much lower than  $T_R$ . Indeed the aspect of a surface on short distances is very similar just below  $T_R$  and just above  $T_R$ . In particular, closed terraces are present between steps, and steps exhibit “overhangs” which are generally ignored in available theoretical treatments. The choice  $T < T_R/2$  seems reasonable. This implies, according to (2.1, 2.5), a second condition on  $\xi$

$$\xi > 3a. \quad (2.6)$$

It turns out that conditions (2.4, 2.6) are not always simultaneously satisfied in simulations, especially when diffusion kinetics is considered. For instance, a typical set of values used by Jiang and Ebner [16] is  $\lambda/a = 40$ ,  $M/a = 32$ ,  $h/a = 5$  initially, at time  $t = 0$ . Then (2.4) yields the acceptable condition  $\xi/a < 8$  at  $t = 0$  and  $\xi/a < 2$  at a later time, when  $h$  is reduced by a factor 2, which is incompatible with (2.6). Moreover, the average distance  $\ell = \lambda a / 4h$  between steps is so short that (1.1) is not acceptable. Erlebacher and Aziz [17] use longer samples, with  $M/a = 256$  and a shorter wavelength  $\lambda \leq 64$  and height  $h(t=0)/a = 4$ . Then (2.4) yields  $\xi/a < 16$  at  $t = 0$  and for  $h/a = 2$ , at a later time,  $\xi/a < 4$ , which is not so good with respect to equation (2.6). Murty and Cooper [18] use longer samples yet, with  $M/a = 1000$ ,  $\lambda \leq 40$  and height  $h(t=0)/a = 4$  too. Now, (2.4) yields  $\xi/a < 160$  at  $t=0$  and  $\xi/a < 40$  when  $h$  is reduced by a factor 2. These conditions are fully consistent with (2.6), and actually Murty and Cooper do find the scaling law  $\tau \simeq \lambda^5$  predicted by Ozdemir and Zangwill. Note, however, the very low value of  $h$  in all simulations. A consequence is an oscillation of the shape, which generally shows alternately a flat top (and bottom) and a sharper top (and bottom).

The conclusion of this section is that, for diffusion kinetics, simulations are not always done in systems which are clearly in the region where analytic theories should apply. The choice of all lengths ( $\lambda$ ,  $h$ ,  $M$ ) results from a compromise between too large values which would saturate computers, and too short sizes which would have no relation with reality.

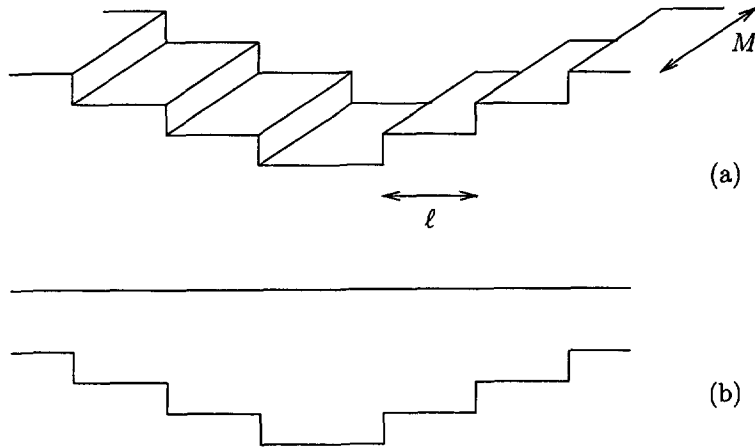


Fig. 2. — A groove cut in a system of width  $M$  smaller than the distance between kinks  $\xi$  (a) and its representation as a groove along a one-dimensional profile (b).

We are then led to study the behaviour of a very narrow system, with a very low value  $M$ , but large values of  $\lambda$  and  $h$ . We thus should obtain, in the very particular case of a narrow system, well-defined informations on the scaling of  $\tau$  versus  $\lambda$ , and on the shape: is the evolution shape-preserving? Are the top and the bottom flat? Another information which is expected is the effect of small values of  $h/a$  and  $\ell/a$ . We thus hope to get an insight into the numerical results obtained for intermediate sizes.

### 3. The One-Dimensional Model

From now on, we consider a short sample, which satisfies the following relation, opposite to (2.4):

$$M \ll \xi \left( \frac{\lambda}{4h} \right)^2 \quad (3.1)$$

On such a sample, the position  $x$  of each step is defined with an accuracy, given by (2.2), which is much better than the distance to the neighbouring steps. We shall therefore replace the model by a one-dimensional one, in which each step has a well-defined position at any time (Fig. 2). Our model is different from the one-dimensional one treated by Searson *et al.* [23]. Indeed, in our model, there are steps which can move by exchanging atoms between themselves or with the vapour, but atoms between steps are not explicitly considered.

In the problem of thermal smoothing, two different types of kinetics are of interest:

- i) The evaporation-condensation kinetics, in which atoms are exchanged between the surface and the vapour, and the total number of evaporated atoms is equal on the average to the total number of condensed atoms.
- ii) The diffusion kinetics, in which evaporation and condensation are negligible, and atoms can only diffuse on the surface. There are several versions [7], and we shall use the “fast attachment version” in which atoms are emitted by steps and stick at a step as soon as they meet one.

We shall come back to evaporation-condensation kinetics in Section 7. In the remainder of the present section, we address the diffusion kinetics.

The one-dimensional model with diffusion kinetics is fully characterized by the probabilities per unit time  $\alpha^+(\ell)$  and  $\alpha^-(\ell)$ , for two steps at distance  $\ell$ , to exchange an atom in one direction or in the other one. The case of two steps of identical sign will be considered first. Consider the configuration  $B$  obtained from a configuration  $A$  by transferring one atom downward from a step to the neighbouring one at distance  $\ell$ . The transition probability per unit time from  $A$  to  $B$  is, by definition,  $\alpha^+(\ell)$ . The transition probability per unit time from  $B$  to  $A$  is  $\alpha^-(\ell + 2a)$  because the terrace width in  $B$  is  $\ell + 2a$ . In the absence of interaction between steps, both configurations  $A$  and  $B$  have the same energy, and the detailed balance relation writes

$$\alpha^-(\ell + 2a) = \alpha^+(\ell). \quad (3.2)$$

One might have expected the different relation  $\alpha^-(\ell) = \alpha^+(\ell)$ . As will be seen in Section 4, the form (3.2) is crucial, but special to one dimension.

*Dependence of  $\alpha^-(\ell)$  and  $\alpha^+(\ell)$  with respect to  $\ell$*

If the distance  $\ell$  between both steps is large, most of the emitted atoms go back to the step where they started from. The transfer probabilities  $\alpha^-(\ell)$  and  $\alpha^+(\ell)$  are therefore expected to decrease with increasing  $\ell$ .

Let  $p(\ell)$  be the probability for an emitted atom to reach the opposite step instead of coming back to the same step. It can be checked that  $p(x) = a/x$ . Indeed, the probability for an atom to come back after having reached the distance  $x$  for the first time from a step is the same as the probability of this atom to reach the distance  $2x$ , and therefore  $p(2x) = p(x)/2$  which is indeed satisfied if  $p(x) = a/x$  which also satisfies the obvious condition  $p(a) = 1$ . Therefore, the probabilities per unit time for two steps at distance  $\ell$  to exchange an atom are expected to be proportional to  $1/\ell$  for large  $\ell$ . More precisely, it can be shown (Appendix A), that:

$$\alpha^+(\ell) = \alpha_0 \frac{a}{\ell + \ell_s + a} \quad (3.3)$$

and

$$\alpha^-(\ell) = \alpha_0 \frac{a}{\ell + \ell_s - a} \quad (3.4)$$

where  $\alpha_0$  is a constant and  $\ell_s$  is a length which depends on the detachment probability of atoms from steps. In our simulations, we have assumed

$$\ell_s = 0 \quad (3.5)$$

which corresponds to equal detachment probabilities upward and downward, *i.e.*, the so-called Ehrlich-Schwoebel effect [21, 22] is absent.

The values (3.3, 3.4) satisfy the detailed balance relation (3.2).

The model can thus be defined in terms of steps only, and atoms can be forgotten. In each pair of neighbouring, isolated steps of identical signs (*i.e.* both steps are upstairs or downstairs) at distance  $\ell$ , the steps are allowed to jump by 1 atomic distance in opposite directions with the probability given by (3.3, 3.4).

In the case of steps of different signs (*i.e.* at the top or at the bottom) the jumps should be in the same direction for both steps, and the possibility of terrace annihilation should be considered. This complication, as well as those arising from step bunches, is addressed in Appendix B.

We ignore the possibility of terrace creation. This is justified at low temperatures and far from equilibrium, *i.e.* for short enough times, when the ratio  $h/\lambda$  is large with respect to the value compatible with thermal roughness.

Before reporting the results of the calculations, we wish to stress the importance of relations (3.3, 3.4), and to precise the relation of the one-dimensional model with reality.

#### 4. A Kinetic, Attractive Interaction

The probability (3.3) to increase the distance is smaller than the probability (3.4) to decrease it. This difference, which is a consequence of the detailed balance relation (3.2), means that the system of steps behaves as if there was an attractive interaction between them .. although (3.2) results from the assumption that there is no interaction!

This astonishing property is responsible for a blunting of the profile; steps of identical sign attract themselves, so that the maximal slope increases, and consequently the top and the bottom flatten.

However, the effective attraction, as described in the previous section, is typical of a one-dimensional system. It will now be argued that it is still expected in a short system (*i.e.* for small  $M$ ) but with a weaker strength. The easiest way to see that is to extend the detailed balance relation (3.2) to the case  $M \neq 1$ . As in the previous section, we can consider a state  $A$  where two particular steps have a distance  $\ell$ , and the state  $B$  deduced from  $A$  by transferring one atom from one step to the other in the downward direction. The average distance between the two steps (which is no longer an integer multiple of the atomic distance  $a$ ) is now increased by an amount  $2a/M$ . If  $\alpha_M^+(\ell)$  and  $\alpha_M^-(\ell)$  denote the transition probability per unit time from  $A$  to  $B$  and from  $B$  to  $A$  respectively, the detailed balance relation is therefore

$$\alpha_M^-(\ell + 2a\frac{a}{M}) = \alpha_M^+(\ell). \quad (4.1)$$

Since we still want  $\alpha_M^-(\ell)$  and  $\alpha_M^+(\ell)$  to be proportional to  $1/\ell$  for large  $\ell$ , it is reasonable to assume that they are given by formulae analogous to (3.3) and (3.4), with the following changes: i)  $a$  is replaced by  $a/M$  in order to satisfy (4.1); ii) the factor  $\alpha_0$  is replaced by  $\alpha_1 M/a$ , where  $\alpha_1$  is the atom emission probability per unit time and per site of the step and  $M/a$  is the number of sites; iii) (3.5) is assumed to hold. We thus obtain

$$\alpha_M^+(\ell) = \alpha_1 \frac{M}{\ell + a^2/M} \quad (4.2)$$

and

$$\alpha_M^-(\ell) = \alpha_1 \frac{M}{\ell - a^2/M}. \quad (4.3)$$

These formulae are the simplest generalizations of (3.3, 3.4), but their validity is not so well established. They express the fact that an adatom which is exchanged between two neighbouring steps has a shorter path to diffuse if it goes up than if it goes down. The difference is exactly  $2a$  on a one-dimensional surface, but it decreases when  $M$  increases. The real behaviour is certainly more complex than (4.2, 4.3), and should depend among other things on the kinetics of kinks on steps. Indeed, in the denominator of (4.2, 4.3), the correction  $a^2/M$  is the averaged recoil of a step which emits an atom. The average is done on the whole step, as would be correct if atom diffusion along a step were infinitely fast. In fact it is not, the correct averaging should be local, and the effective attraction presumably does not vanish for infinite  $M$ , as would be expected from (4.2, 4.3).

The effective attraction between steps, described in this section, is a purely kinetic effect, which does not violate the laws of Physics. It has no effect on the thermodynamic properties. For instance, the equilibrium probabilities of two step configurations with identical energies are equal, and not affected by the kinetic attraction. Indeed, this equality can be derived from the detailed balance principle, which is also the source of the effective attraction derived above.

Moreover, the effective interaction vanishes in the continuum limit  $a = 0$  as readily seen from (4.2, 4.3).

Formulae (4.2, 4.3) will now allow us to relate the basic parameter  $\alpha_0$  of the one-dimensional model, which appears in (3.3, 3.4), to the physical parameter  $\alpha_1$ .

## 5. Relation between the One-Dimensional Model and Reality

In order to simplify the argument, it is appropriate to focus the attention on a pair of steps and to ignore the atoms they exchange with the other steps. The generalization will be straightforward.

In order to exploit the atom exchange probabilities in the one-dimensional model and in the physical one, it is appropriate to introduce the net number of atoms  $n$  transferred from the upper step to the lower step after a time  $t$ . This number can be positive or negative and a variation of  $\delta n$  implies a variation of  $\ell$  equals to

$$\delta\ell = 2\delta n a^2 / M. \quad (5.1)$$

For a short bidimensional system of width  $M$ , the probability  $p_M(\ell, t)$  that  $\ell$  has a particular value at time  $t$  obeys the master equation:

$$\begin{aligned} \frac{\partial}{\partial t} p_M(\ell, t) = & - [\alpha_M^+(\ell) + \alpha_M^-(\ell)] p_M(\ell, t) \\ & + \alpha_M^+(\ell - 2a^2/M) p_M(\ell - 2a^2/M, t) \\ & + \alpha_M^-(\ell + 2a^2/M) p_M(\ell + 2a^2/M, t). \end{aligned} \quad (5.2)$$

Using the detailed balance relation (4.1), formula (5.2) can be written

$$\begin{aligned} \frac{\partial}{\partial t} p_M(\ell, t) = & \alpha_M^+(\ell) [p_M(\ell + 2a^2/M, t) - p_M(\ell, t)] \\ & + \alpha_M^-(\ell) [p_M(\ell - 2a^2/M, t) - p_M(\ell, t)]. \end{aligned} \quad (5.3)$$

If  $\ell$  is regarded as a continuous variable and if  $p_M(\ell, t)$  is assumed to be a twice differentiable function of  $\ell$ , relation (5.3) yields

$$\frac{\partial}{\partial t} p_M(\ell, t) = \frac{2a^2}{M} [\alpha_M^+(\ell) - \alpha_M^-(\ell)] \frac{\partial}{\partial \ell} p_M(\ell, t) + \frac{2a^4}{M^2} [\alpha_M^+(\ell) + \alpha_M^-(\ell)] \frac{\partial^2}{\partial \ell^2} p_M(\ell, t). \quad (5.4)$$

Insertion of (4.2) and (4.3) into (5.4) yields, if  $\ell^2 - a^4/M^2 \simeq \ell^2$ ,

$$\begin{aligned} \frac{\partial}{\partial t} p_M(\ell, t) = & -4\alpha_1 \frac{a^4}{M\ell^2} \frac{\partial}{\partial \ell} p_M(\ell, t) + 4\alpha_1 \frac{a^4}{M\ell} \frac{\partial^2}{\partial \ell^2} p_M(\ell, t) \\ \frac{\partial}{\partial t} p_M(\ell, t) = & 4\alpha_1 \frac{a^4}{M} \frac{\partial}{\partial \ell} \left[ \frac{1}{\ell} \frac{\partial}{\partial \ell} p_M(\ell, t) \right]. \end{aligned} \quad (5.5)$$



In the one-dimensional model defined in section 3, the probability  $p_1(\ell, t)$  satisfies an equation analogous to (5.5). In the derivation,  $M$  should be replaced by  $a$ , and the relations (4.1, 4.2, 4.3) should be replaced by (3.2, 3.3, 3.4):

$$\frac{\partial}{\partial t} p_1(\ell, t) = 4\alpha_0 a^3 \frac{\partial}{\partial \ell} \left[ \frac{1}{\ell} \frac{\partial}{\partial \ell} p_1(\ell, t) \right]. \quad (5.6)$$

The equations satisfied in the one-dimensional model and in the physical one are therefore the same if

$$\alpha_0 = \alpha_1 \frac{a}{M}. \quad (5.7)$$

In the above derivation, we have considered a set of two steps. However, the general evolution equation can be obtained by combining all equations of type (5.5) corresponding to all pairs of neighbouring steps, and the rule (5.7) is therefore general.

## 6. Calculations

At  $t = 0$ , the profile is described by the function:

$$f(x) = h_0 \sin \left( \frac{2\pi x}{\lambda} \right) \quad (6.1)$$

where  $\lambda$  is the wavelength and  $h_0$  is the initial profile amplitude. The discretization of the profile is given by the relation:

$$h(i, 0) = \text{Nint} \left( f \left( i + \frac{1}{2} \right) \right) \quad i \in [0, \lambda - 1] \quad (6.2)$$

where  $h(i, 0)$  is the altitude between  $i$  and  $i + 1$  at  $t = 0$  and, in order to be as close as possible of the initial curve, we use the function Nint, which rounds a real to the closest integer.

We impose periodic boundary conditions with a period equal to  $\lambda$ .

The attachment and detachment of particles can only occur at the corners of the profile (Fig. 3a). We made the distinction between corners and steps since the existence of macrosteps (for instance double steps) is allowed (Appendix B). We call the corners which "point outside the surface" the possible donors of the configuration. On the other hand the possible acceptor locations are the corners which "point inside the surface". Due to the detachment or attachment of a packet of atoms ("particle"), each step can move to its left or to its right. For diffusion dynamics, the particle has to travel along a distance  $\ell$  between donor and acceptor.

We performed a Kinetic Monte Carlo simulation [24] defined by the following algorithm:

- At a given time  $t$ , one has to determine all the possible events, *i.e.* all sites which can be donors and all the possible displacements (right and left). We calculate their lengths  $\ell_i^\varepsilon$  (where  $i$  represents the donor and  $\varepsilon$  the direction), their probability per unit time  $\alpha(\ell_i^\varepsilon)$  (given by Eqs. (3.3, 3.4)) and the sum of all those probabilities per unit time,  $\alpha = \sum_{i,\varepsilon} \alpha(\ell_i^\varepsilon)$ .

- We increment the time by a lifetime  $\tau$  of the profile which is a random number distributed as

$$\rho(\tau) = \alpha \exp(-\alpha\tau). \quad (6.3)$$

- We choose the event which occurs with probability  $\alpha(\ell_i^\varepsilon)/\alpha$ . This event changes the profile for a new iteration.

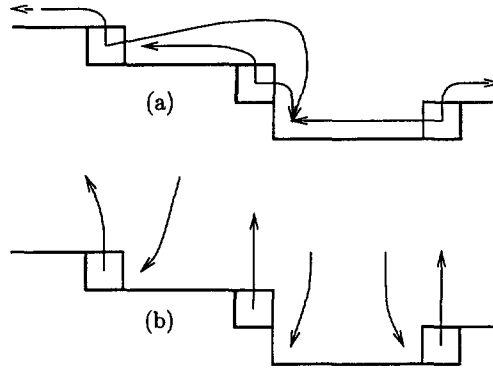


Fig. 3. — Mechanism of diffusion and evaporation-condensation. Figure (a) displays all the possible displacements by diffusion. All those events are independent, and their probabilities depend on the length of the displacement. In Figure (b), we have the same configuration but the mechanism is evaporation-condensation. The six events are independent and occur with the same probability.

We stress that the detailed balance relation is satisfied in the general case since we use equations (3.3, 3.4) for the transition rates and also in the particular cases of top and bottom terraces, as addressed in Appendix B.

Calculations have been performed with  $h_0 = 10$  and  $20$  and  $\lambda = 200$  to  $600$  to determine the scaling properties. To characterize the time evolution of the profile, we have performed averages over  $N$  different realizations starting from the same initial profile.

The averaged altitude is given by:

$$h(i, t) = \frac{1}{N} \sum_{n=1}^N h_n(i, t). \tag{6.4}$$

One can define the amplitude of the profile for the realization  $n$  by

$$h_n(t) = \frac{1}{2} \left( \max_i(h_n(i, t)) - \min_i(h_n(i, t)) \right) \tag{6.5}$$

and its average:

$$h(t) = \frac{1}{N} \sum_{n=1}^N h_n(t). \tag{6.6}$$

Figure 5 displays the averaged profiles, *i.e.*, the altitude  $h(x, t)$  versus  $x$ , for different times. We observe that after a short transient, the profiles exhibit maxima and minima which are flatter than a sinusoid. This is the signature of the presence of facets which can be seen directly on each profile in Figure 4; these facets have been already observed by Jiang and Ebner [16] for a (2+1) SOS model. When the amplitude  $h(t)$  becomes smaller, of the order of  $h_0/3$ , the broadening is less pronounced, but still exists.

Figure 6 displays the evolution of the amplitude with scaled times  $t/\lambda^3$  for three different wavelengths  $\lambda$  and two initial amplitudes  $h_0$ . The observed scaling behaviour agrees with the theoretical prediction (Appendix C). We observe that for sufficiently large initial ratios  $\lambda a/4h_0$  (this implies relatively large values of the distance  $\ell$  between steps, say  $\ell > 4a$ ), the scaling is really perfect. However, if we consider too large amplitudes which imply  $\ell \approx a$ , the scaling can be affected.

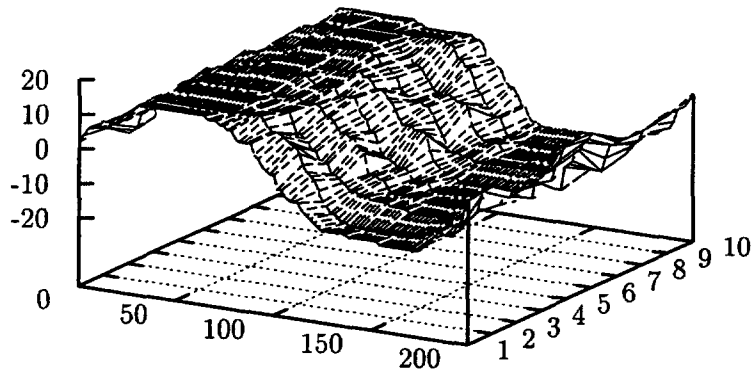


Fig. 4. — Diffusion mechanism: profile for ten realizations without averaging. This figure exhibits real facets. Making averages over many realizations smooths the profile and hide the sharp angles.

## 7. Evaporation-Condensation Kinetics

In the case of evaporation-condensation kinetics, the relevant quantities for the one-dimensional model are the probabilities per unit time  $\gamma^e$  and  $\gamma^c$ , for a step to exchange an atom with the vapour, respectively by evaporation and condensation. Consider the configuration  $B$  obtained from a configuration  $A$  by evaporating one atom from a step to the vapour.

The transition probability per unit time from  $A$  to  $B$  is, by definition,  $\gamma^e$ . The transition probability per unit time from  $B$  to  $A$  is  $\gamma^c$ . Since the energies of both configurations are equal if we neglect interactions between the atom and the surface, the detailed balance relation writes

$$\gamma^e = \gamma^c = \gamma_0 \quad (7.1)$$

where  $\gamma_0$  is a constant.

For a short system (with small  $M$ ), we can consider a state  $A$  and the state  $B$  deduced from  $A$  by evaporating one atom from a step to the vapour. If  $\gamma_M^e$  and  $\gamma_M^c$  denote the transition probability per unit time from  $A$  to  $B$  and from  $B$  to  $A$  respectively, the detailed balance relation is therefore

$$\gamma_M^e = \gamma_M^c = \gamma_1 M/a \quad (7.2)$$

where  $\gamma_1$  is the atom evaporation-condensation probability per unit time and per site of the step and  $M/a$  is the number of sites along the step.

Now we will relate the basic parameter  $\gamma_0$  of the one-dimensional model to the physical parameter  $\gamma_1$ , in an analogous way as it was done for the diffusion dynamics, but in the present case the transition rates do not depend on  $\ell$ .

As before, we focus the attention on a pair of neighbouring steps of identical signs separated by a distance  $\ell$  and ignore the others. For a short bidimensional system of width  $M$ , the probability  $p_M(\ell, t)$  that  $\ell$  has a particular value at time  $t$  obeys the master equation:

$$\begin{aligned} \frac{\partial}{\partial t} p_M(\ell, t) &= -[2\gamma_M^e + 2\gamma_M^c] p_M(\ell, t) \\ &+ [\gamma_M^e + \gamma_M^c] p_M(\ell - a^2/M, t) \\ &+ [\gamma_M^c + \gamma_M^e] p_M(\ell + a^2/M, t). \end{aligned} \quad (7.3)$$

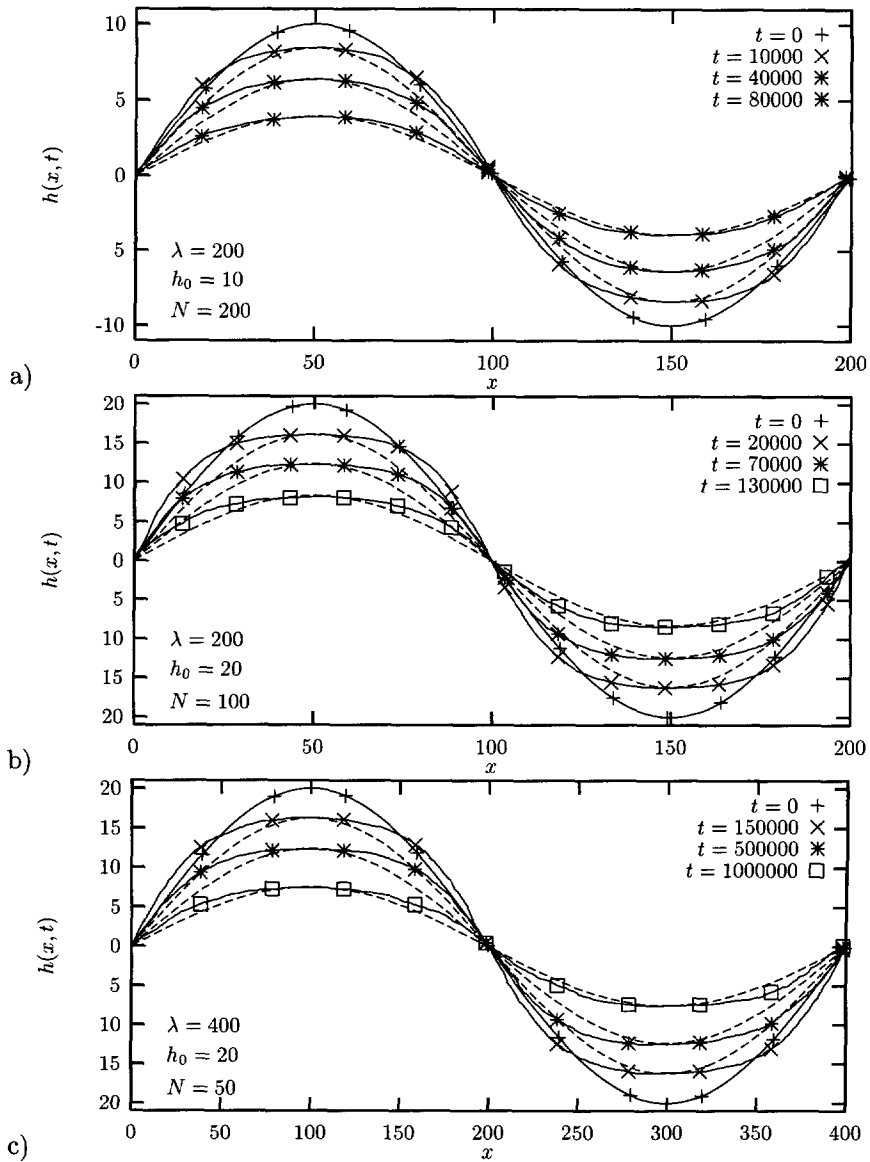


Fig. 5. — Diffusion mechanism: average profile *versus* the position  $x$  for different times. For all times, sinusoids have been superimposed.  $N$  is the number of realizations for each size.

Using the detailed balance relation (7.2), and under the same assumptions as before for diffusion, formula (7.3) can be written

$$\frac{\partial}{\partial t} p_M(\ell, t) = 2\gamma_1 \frac{a^3}{M} \frac{\partial^2}{\partial \ell^2} p_M(\ell, t). \tag{7.4}$$

For the one-dimensional model, the probability  $p_1(\ell, t)$  satisfies an equation analogous to (7.4).

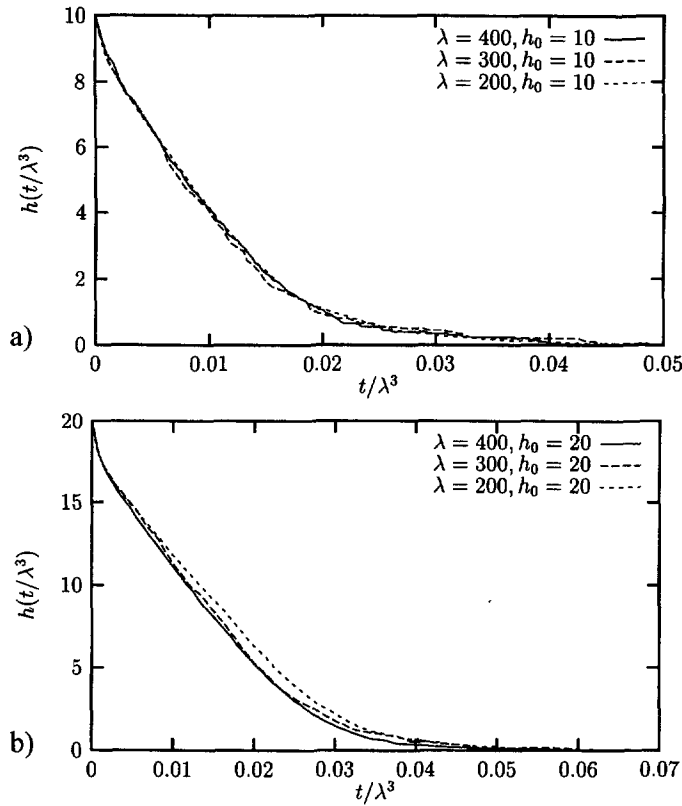


Fig. 6. — Diffusion mechanism: averaged amplitude  $h(t)$  as a function of time. For  $\lambda = 200, h_0 = 20$ , the condition  $\lambda/4h_0 \gg 1$  is not well satisfied ( $\lambda/4h_0 = 2.5$ ) and the scaling is not so good as for other sizes.

In the derivation,  $M$  should be replaced by  $a$ , and the relation (7.2) should be replaced by (7.1):

$$\frac{\partial}{\partial t} p_1(\ell, t) = 2\gamma_0 a^2 \frac{\partial^2}{\partial \ell^2} p_1(\ell, t). \tag{7.5}$$

The equations satisfied in the one-dimensional model and in the physical one are therefore the same if

$$\gamma_0 = \gamma_1 \frac{a}{M}. \tag{7.6}$$

As before, the general evolution equation can be obtained by combining all equations of type (7.4) corresponding to all pairs of neighbouring steps, and the rule (7.6) is therefore general.

The steps can then be seen as particles which can now jump independently (except when they are in contact), with the same jumping rate, in a one-dimensional medium. Steps of opposite signs annihilate when they get in contact. This model has been studied in detail by Galfi and Racz [25] and by Leyvraz and Redner [26]. However, since our initial conditions are rather special and the problem is fairly simple, we have done our own computations.

The initial profile and discretization are the same as for diffusion (Sect. 6). We also considered periodic boundary conditions. The particles which can evaporate and the sites which can receive a particle by condensation are represented in Figure 3b.

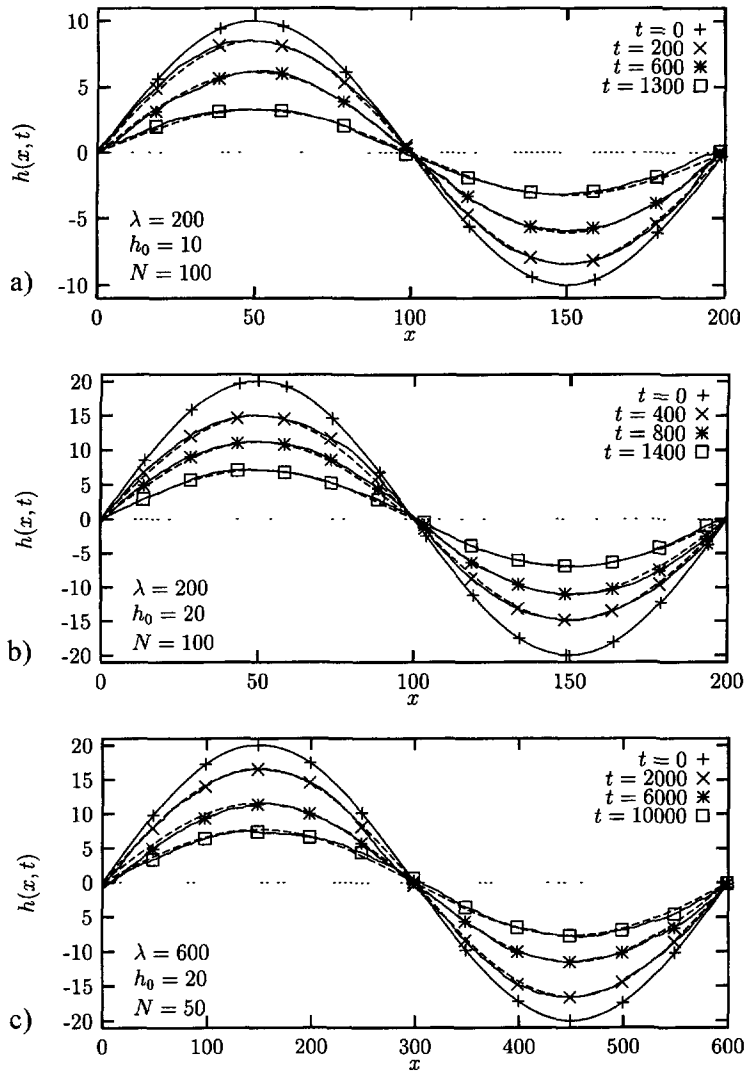


Fig. 7. — Evaporation-condensation mechanism: averaged profile *versus* the position  $x$  for different times. For all times, a sinusoid has been superimposed.  $N$  is the number of realizations for each size.

In a given configuration, all events (evaporation and condensation) have the same probability.

The kinetic Monte Carlo algorithm is the same as for diffusion. We have displayed our results in Figures 7 and 8.

Figure 7 displays the profile as a function of time. We can see that the profile remains sinusoidal during the relaxation, in contrast with the relaxation through diffusion.

In Figure 8, we have displayed the amplitude *versus* time for three values of the wavelength. The scaling law is found to be in  $t/\lambda^2$  (see Appendix C). For the amplitude  $h(t)$ , the fit with the function  $h_0 \exp(-\alpha t/\lambda^2)$  is found to be in very good agreement with our data.

It is interesting to note that our results are different from the results found by Tang [27] since his simulation, for large and long samples, belongs to a different situation than the one

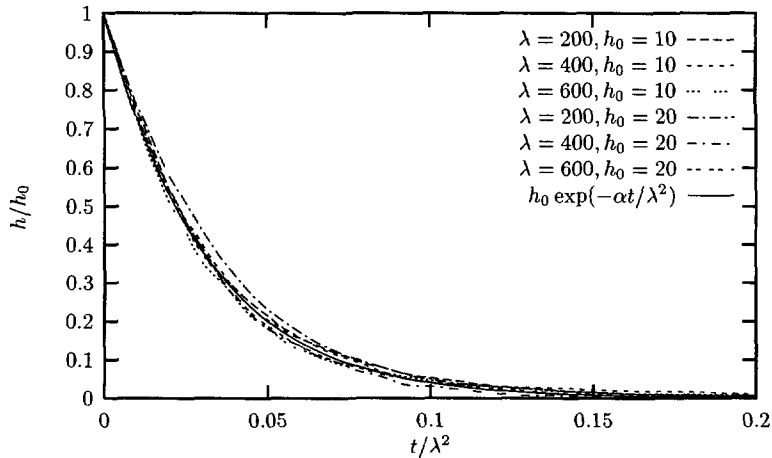


Fig. 8. — Evaporation-condensation mechanism: averaged amplitude as a function of time. For all sizes and amplitudes, there is an excellent fit of  $h(t)/h_0$  with the function  $\exp(-\alpha t/\lambda^2)$  where  $\alpha$  is an adjustable parameter ( $\alpha = 32 \pm 0.5$ ).

considered in this paper. For instance, Tang considers grooves of wavelength  $\lambda = 300a$ , width  $M = 19\,200a/\sqrt{3}$  and initial amplitude  $h_0 = 15a$ . His simulation results, for evaporation kinetics, are compatible with a relaxation time scaling in  $\lambda^3$  and the profiles obtained are sharper than a sinusoid at the top and the bottom but have more rounded shapes than the ones predicted by Lançon and Villain [10].

## 8. Conclusion

The thermal smoothing of a grooved, high-symmetry surface below its roughening transition is considered. To compare the mean field theoretical predictions (which consider the entropic interaction between steps), with the simulation results using the SOS model in  $(2+1)$  dimensions, two conditions over the distance  $\xi$  between kinks along the steps must be satisfied:  $\xi \ll M(4h/\lambda)^2$  and  $\xi > 3a$  (temperature  $T < T_R/2$ ). These two conditions are not always simultaneously satisfied in the simulations, since they are restricted (due to the slow diffusion dynamics) to samples which are in general too small in the three directions.

We then introduced a model to study the relaxation of a profile which mimics a very narrow two-dimensional system at temperatures  $T < T_R$ . The atomic diffusion is treated as effective jumps between steps (which occur with an appropriated probability) in order to save time in our simulations and then allow us to consider greater amplitudes  $h_0$  and longer systems.

There are two main contributions in this paper. On one hand, kinetic Monte Carlo simulations have been done on profiles which have a reasonably large amplitude  $h_0$  and wavelength  $\lambda$ , but a very short width  $M$ , in contrast with usual simulations where  $M$  is moderately large (not always enough) but  $h_0$  is too small. On the other hand, a new kinetic, attractive interaction between steps has been evidenced, and its effect has been found to be important. This interaction is particularly strong on a one-dimensional surface, but should not vanish on a physical surface.

The most remarkable effect of the attractive interaction is a blunting of the profile, *i.e.* the top and the bottom of the profile are flatter than those of a sinusoid. This effect seems to have been observed in standard Monte Carlo simulations [16]. Thus, our work sheds light

on the effect of too small sizes in simulations. However the scaling of the relaxation time  $\tau$  with the wavelength  $\lambda$  ( $\tau \propto \lambda^2$  for evaporation dynamics and  $\tau \propto \lambda^3$  for diffusion dynamics) does not correspond to those obtained for finite  $M$  by other authors. Instead, the exponent 4 obtained by Jiang and Ebner for diffusion dynamics is intermediate between the exponent 3 obtained here for  $M = 1$  and the exponent 5 valid for  $M = \infty$  [7, 18]

The relevance of the present results for experiments is questionable. Firstly, real samples are often miscut [10, 11]. Secondly, elastic and electrostatic interactions are important in real systems, and neglected, to our knowledge, in all simulations. The edges of a top or bottom terrace are coupled by these interactions, and this coupling may have a strong effect on the transient profile shape. This effect is not generic, but depends on the nature of the coupling, which may be attractive or repulsive. This problem will be addressed in another article.

## Acknowledgments

We gratefully acknowledge Prof. B. Derrida for fruitful discussions. A.C. acknowledges a grant from the Brazilian National Council for the Scientific and Technological Development (CNPq) and the hospitality of the Centre d'Études Nucléaires de Grenoble.

## Appendix A

### Derivation of $\alpha^+(\ell)$ and $\alpha^-(\ell)$

Consider the system composed by two steps shown in Figure 9. In order to have a steady state, we impose that every particle reaching the position  $\ell/a + 1$  is immediately placed at position 0.

Let  $p_i(t)$  be the probability for an atom to be at position  $i$  for  $i \in [1, L = \ell/a]$ . The probabilities  $\{p_i(t)\}$  satisfy Master equations:

$$\begin{aligned} \frac{\partial}{\partial t} p_1(t) &= \alpha - \alpha' p_1(t) - \alpha_1 p_1(t) + \alpha'_1 p_2(t) \\ \frac{\partial}{\partial t} p_2(t) &= \alpha_1 p_1(t) - \alpha'_1 p_2(t) - \alpha_2 p_2(t) + \alpha'_2 p_3(t) \\ \frac{\partial}{\partial t} p_{L-1}(t) &= \alpha_{L-2} p_{L-2}(t) - \alpha'_{L-2} p_{L-1}(t) - \alpha_{L-1} p_{L-1}(t) + \alpha'_{L-1} p_L(t) \\ \frac{\partial}{\partial t} p_L(t) &= \alpha_{L-1} p_{L-1}(t) - \alpha'_{L-1} p_L(t) - \gamma p_L(t). \end{aligned}$$

Since the system is in a steady state all those time derivatives must be equal to zero. Hence:

$$\begin{aligned} \alpha^+(\ell) &= \gamma p_L \\ &= \alpha_{L-1} p_{L-1} - \alpha'_{L-1} p_L \\ &= \alpha_{L-2} p_{L-2} - \alpha'_{L-2} p_{L-1} \\ &= \alpha_1 p_1 - \alpha'_1 p_2 \\ &= \alpha - \alpha' p_1. \end{aligned}$$



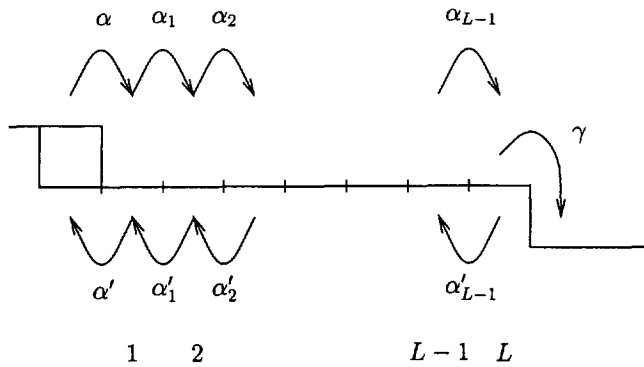


Fig. 9. — Notations for Appendix A.

Through a recurrence procedure one then obtains that:

$$\alpha^+(\ell) \left[ 1 + \frac{\gamma}{\alpha'_{L-1}} + \frac{\alpha_{L-1}}{\alpha'_{L-1} \alpha'_{L-2}} \frac{\gamma}{\alpha'_{L-2}} + \dots + \frac{\alpha_{L-1} \dots \alpha_1}{\alpha'_{L-1} \alpha'_1} \frac{\gamma}{\alpha'} \right] = \gamma \frac{\alpha_{L-1} \dots \alpha_1 \alpha}{\alpha'_{L-1} \alpha'_1 \alpha'}. \quad (\text{A.1})$$

(A.1) is a little complicated in the general case, and we will consider a simpler one.

- We assume that, for diffusion, all site energies are equal on the terrace except for  $i = 0$  and  $L + 1$ , thus the detailed balance relations give:

$$\alpha_i = \alpha'_i \quad \forall i \in [1, L - 1]. \quad (\text{A.2})$$

(A.1) becomes

$$\alpha^+(\ell) \left[ 1 + \frac{\gamma}{\alpha_{L-1}} + \frac{\gamma}{\alpha_{L-2}} + \dots + \frac{\gamma}{\alpha_1} + \frac{\gamma}{\alpha'} \right] = \gamma \frac{\alpha}{\alpha'}. \quad (\text{A.3})$$

- The second hypothesis is that all the barrier energies for the diffusion are equal, *i.e.*

$$\alpha_1 = \dots = \alpha_i = \dots = \alpha_{L-1} \quad (\text{A.4})$$

and then (A.3) yields

$$\alpha^+(\ell) \left[ 1 + \left( \frac{\ell}{a} - 1 \right) \frac{\gamma}{\alpha_1} + \frac{\gamma}{\alpha'} \right] = \gamma \frac{\alpha}{\alpha'}. \quad (\text{A.5})$$

Multiplying (A.5) by  $\frac{\alpha_1}{\gamma} a$ ,

$$\alpha^+(\ell) \left[ \ell + a + a \left( \frac{\alpha_1}{\gamma} + \frac{\alpha_1}{\alpha'} - 2 \right) \right] = \alpha_1 \frac{\alpha}{\alpha'} a. \quad (\text{A.6})$$

An analogous calculation gives

$$\alpha^-(\ell + 2a) \left[ \ell + a + a \left( \frac{\alpha_1}{\alpha'} + \frac{\alpha_1}{\gamma} - 2 \right) \right] = \alpha_1 \frac{\gamma'}{\gamma} a. \quad (\text{A.7})$$

If the site 0 and  $L + 1$  have the same energy, the detailed balance relation  $\alpha^+(\ell) = \alpha^-(\ell + 2a)$  is verified if

$$\alpha\gamma = \alpha'\gamma' \quad (\text{A.8})$$

and (A.6, A.7) can be written

$$\alpha^+(\ell) = \alpha_0 \frac{a}{\ell + a + \ell_s} \quad (\text{A.9})$$

$$\alpha^-(\ell) = \alpha_0 \frac{a}{\ell - a + \ell_s} \quad (\text{A.10})$$

with

$$\alpha_0 = \alpha_1 \frac{\alpha}{\alpha'} = \alpha_1 \frac{\gamma'}{\gamma} \quad (\text{A.11})$$

$$\ell_s = a \left( \frac{\alpha_1}{\alpha'} + \frac{\alpha_1}{\gamma} - 2 \right). \quad (\text{A.12})$$

## Appendix B

### Complications Arising from Top and Bottom Terraces and Step Bunches

The case where we consider donor/acceptor steps at the top or at the bottom of the profile requires special attention, since terrace annihilation can occur.

Consider a top (or a bottom) terrace of width  $\ell$ . If  $\ell \geq 2a$ , an atom can be exchanged from one side to the other side of the terrace. In this case, the terrace width is the same for both initial and final configurations and, since they have the same energy, the detailed balance relation in this particular case is written

$$\alpha^{\text{right}}(\ell) = \alpha^{\text{left}}(\ell). \quad (\text{B.1})$$

If the width is minimal,  $a$ , the top terrace represents an entire row of atoms and the energy of this configuration  $A$  is very high. Let us consider the configuration  $B$  where this terrace has disappeared, the detailed balance relation is written

$$\exp(-\beta E_A)\alpha(A \rightarrow B) = \exp(-\beta E_B)\alpha(B \rightarrow A). \quad (\text{B.2})$$

Since  $E_A$  is very high, we assume  $\alpha(B \rightarrow A) = 0$  to satisfy the detailed balance relation and we do not allow the creation of a new terrace (one row of atoms) above the top one (and the similar situation for the bottom terrace), since the energetic cost to move simultaneously an entire row of atoms is too high as soon as  $M$  is larger than a few atomic distances.

The physical reason for the annihilation of a terrace of minimal width is that, if we think in terms of the surface, when two steps (which can fluctuate) touch each other, a region of different curvature (and therefore, different chemical potential) is created (a step "loop"). In this region the detachment of atoms is favoured in comparison with the attachment. The whole terrace will disappear and its mass will, in principle, be distributed to the next neighbours. In our procedure this mass distribution is not done, the terrace (in reality a row) of minimal width is removed as a whole and attached to a neighbouring step. At the end this deficiency is compensated by the average over several runs of the program, and this can be seen through the shape of the averaged relaxation profile, which exhibits a right-left symmetry. Similarly, if the acceptor step limits a bottom terrace (groove) with minimal width, this terrace can also disappear. Indeed, when the bottom groove is interrupted (filled) at some region, this will

create a region of different curvature (and of different chemical potential) where the attachment of other atoms will be favoured. At the end this groove will be completely filled.

In the simulations it is also necessary to take into account the formation of macrosteps in the profile, *i.e.*, more than one step at a given position, a double step for instance.

In a macrostep only the highest step can be chosen as a possible donor of a packet of atoms to another step, otherwise an overhang will be created in the profile, a situation we do not consider here. Furthermore, jumps along macrosteps must be allowed, otherwise the atoms are not able to go down and the macrostep would remain as a stable structure. The inverse movement (climbing of a macrostep) must also be allowed if we want to respect the detailed balance principle.

The existence of macrosteps then implies that we have to precise carefully what steps we can choose for donors and acceptors. The following definitions are used in the program: donors are the corners of the profile which point outside the surface, acceptors are the corners which point inside.

In order to evaluate the total distance  $\ell$  an atom has to diffuse from the donor to the acceptor, it is necessary to consider carefully also the vertical distance along the possible macrostep in between.

## Appendix C

### Dependence on the Period

Consider a system of  $\nu$  parallel steps. Let  $p(\ell_1, \ell_2, \dots, \ell_\nu, t) d\ell_1 \dots d\ell_\nu$  be the probability that the distances between steps have the values  $\ell_1, \ell_2, \dots, \ell_\nu$  at time  $t$ . In the case of surface diffusion dynamics, if these distances are large enough (and in particular if there are no multiple steps) the probability satisfies the following equation which generalizes (5.5):

$$\frac{\partial}{\partial t} p(\ell_1, \ell_2, \dots, \ell_\nu, t) = 4\alpha_1 \frac{a^4}{M} \sum_{r=1}^{\nu} \frac{\partial}{\partial \ell_r} \left[ \frac{1}{\ell_r} \frac{\partial}{\partial \ell_r} p(\ell_1, \ell_2, \dots, \ell_\nu, t) \right]. \quad (\text{C.1})$$

If  $p(\ell_1, \ell_2, \dots, \ell_\nu, t)$  is a solution of (C.1), another solution is  $k^\nu p(k\ell_1, k\ell_2, \dots, k\ell_\nu, k^3 t)$ , where  $k$  is any positive number. In other words, one can consider at time  $t = 0$  two systems with the same number  $\nu$  of steps but two different periods,  $\lambda$  and  $\lambda_k = k\lambda$ , which are similar in the sense that the step positions are

$$x_m(t = 0)$$

and

$$x_{m,k}(t = 0) = kx_m(t = 0).$$

Then the probability that the first system has step distances  $\ell_1, \ell_2, \dots, \ell_\nu$  at time  $t$  will be the same as the probability that the second system has step distances  $k\ell_1, k\ell_2, \dots, k\ell_\nu$  at time  $k^3 t$ . This implies that, if the relaxation time of the first system is  $\tau$ , the relaxation time of the second system is  $k^3 \tau$ . Therefore, the relaxation time is proportional to the *cube* of the wavelength.

Similarly, in the case of evaporation dynamics the probability  $p(\ell_1, \ell_2, \dots, \ell_\nu, t) d\ell_1 \dots d\ell_\nu$  satisfies the following equation which generalizes (7.4):

$$\frac{\partial}{\partial t} p(\ell_1, \ell_2, \dots, \ell_\nu, t) = 2\gamma_1 \frac{a^3}{M} \sum_{r=1}^{\nu} \frac{\partial^2}{\partial \ell_r^2} [p(\ell_1, \ell_2, \dots, \ell_\nu, t)]. \quad (\text{C.2})$$

If  $p(\ell_1, \ell_2, \dots, \ell_\nu, t)$  is a solution of (C.2), another solution is  $k^\nu p(k\ell_1, k\ell_2, \dots, k\ell_\nu, k^2 t)$ , where  $k$  is any positive number.

This implies that for the evaporation dynamics the relaxation time is proportional to the *square* of the wavelength.

## References

- [1] Blakely J.M. and Mykura H., *Acta Metall.* **10** (1962) 565.
- [2] Bonzel H.P., Preuss E. and Steffen B., *Appl. Phys. A* **35** (1984) 1.
- [3] Bonzel H.P., Preuss E. and Steffen B., *Surf. Sci.* **145** (1984) 20.
- [4] Bonzel H.P., Breuer U., Voigtländer B. and Zeldov E., *Surf. Sci.* **272** (1992) 10.
- [5] Mullins W.W., *J. Appl. Phys.* **28** 333 (1957); **30** (1959) 77.
- [6] Rettori A. and Villain J., *J. Phys. France* **49** (1988) 257.
- [7] Ozdemir M. and Zangwill A., *Phys. Rev. B* **42** (1990) 5013.
- [8] Spohn H., *J. Phys. I France* **3** (1993) 69.
- [9] Hager J. and Spohn H., *Surf. Sci.* **324** (1995) 365.
- [10] Lançon F. and Villain J., in "Kinetics of Ordering and Growth at Surfaces", M.J. Lagally, Ed. (Plenum Press, New York, 1990).
- [11] Bonzel H.P. and Mullins W.W., *Surf. Sci.* **350** (1996) 285.
- [12] Gruber E.E. and Mullins W.W., *J. Phys. Chem. Solids* **28** (1967) 875.
- [13] Haldane F.D.M. and Villain J., *J. Phys.* **42** (1981) 1673.
- [14] Selke W. and Duxbury P.M., *Phys. Rev. B* **52** (1995) 17468.
- [15] Jiang Z. and Ebner C., *Phys. Rev. B* **40** (1989) 316.
- [16] Jiang Z. and Ebner C., *Phys. Rev. B* **53** (1996) 11146.
- [17] Erlebacher J.D. and Aziz M.J., *Surf. Sci.* **374** (1997) 427.
- [18] Ramana Murty M.V. and Cooper B.H., *Phys. Rev. B* **54** (1996) 10377.
- [19] Villain J., in "Ordering in strongly fluctuating condensed matter systems", T. Riste, Ed. (Plenum Press, New York, 1980).
- [20] Fisher M.E. and Fisher D.S., *Phys. Rev. B* **25** (1982) 3192.
- [21] Ehrlich G. and Hudda F.G., *J. Chem. Phys.* **44** (1966) 1039.
- [22] Schwoebel R.L. and Shipsey E.J., *J. Appl. Phys* **37** (1966) 3682; Schwoebel R.L., *J. Appl. Phys* **40** (1969) 614.
- [23] Searson P.C., Li R. and Sieradzki K., *Phys. Rev. Lett.* **74** (1995) 1395.
- [24] Bortz A.B., Kalos M.H. and Lebowitz J.L., *J. Comp. Phys.* **17** (1975) 10.
- [25] Gálfi L. and Rácz Z., *Phys. Rev. A* **38** (1988) 3151.
- [26] Leyvraz F. and Redner S., *Phys. Rev. Lett.* **66** (1991) 2168.
- [27] Tang L.H., in Dynamics of Crystal Surfaces and Interfaces, P.M. Duxbury and T. Pence, Eds. (Plenum Press, New York, 1997).